# Similarity of Turbulent Wall Fires

J. L. de RIS, G. H. MARKSTEIN, L. ORLOFF and P. A. BEAULIEU
FM Global Research
Norwood, MA 02062, USA

## ABSTRACT

The study establishes a similarity relationship controlling the buoyant turbulent boundary layer combustion of wall fires. Measurements of soot deposition onto glass rods allow one to infer the characteristic thickness, $\delta_S$, of propylene flames at different heights, $z$, and mass transfer rates, $\dot{m}''$. The normalized flame thickness, $\delta_S/z$, is successfully correlated by the overall fuel to air mass ratio of the flames, $\Psi$. Similarly, $\Psi$, correlates the measured boundary layer temperature profiles of the flames normal to the wall. It correlates measurements of the outward directed radiance, $N_r$ from the same propylene wall fires with a uniform effective flame radiation temperature, $T_f$, and uniform soot absorption/emission coefficient being independent of both height, $z$, and fuel mass transfer rate, $\dot{m}''$. Finally the same fuel to air ratio, $\Psi$, correlates, here for the first time, the LDV velocity measurements of Most et al for turbulent ethane wall flames performed at Factory Mutual Research in 1982. The data presented here are suitable for development of analytical and CFD models of turbulent wall fires.

**KEY WORDS:** Turbulent Diffusion Flames, Wall Fires, Flame Radiation, Flame Heat Transfer

## INTRODUCTION

The overall objective is the development of models predicting the total heat transfer from the flames to the wall in both the pyrolysis and forward heat transfer zones of a spreading fire. The present study focuses on the pyrolysis zone supplying fuel to the fire. Figure 1, shows the burner used to study two-dimensional burning of a single wall. This is the simplest wall geometry for studying buoyant boundary layer mixing and combustion. A goal is to identify a fundamental similarity parameter that controls the buoyant fluid mechanics and turbulent combustion, but is insensitive to fuel chemistry. Having found such a parameter, one can then focus on the fuel without being distracted by the fluid

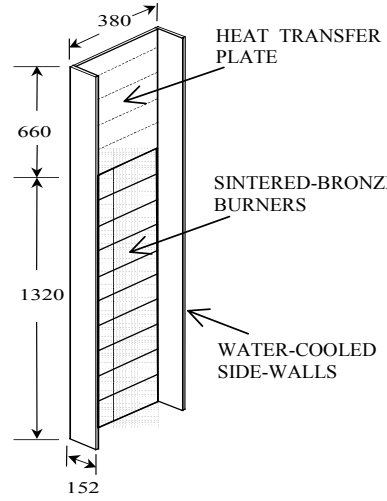


**Figure 1. Gas Burner Apparatus**

mechanics. The fuel mass transfer, $\dot{m}''$, emerges uniformly from all active water-cooled sintered-metal burners. Each burner measures 132 mm high and 380 mm wide resulting in an overall height of 1320 mm for the ten burners. The apparatus is certainly large enough to achieve fully turbulent flames. The 152 mm deep water-cooled sidewalls maintain the flow as two-dimensional. Further details of the apparatus are available[1,2,3].

## SOOT DEPTH

Our first task is to characterize the thickness of the luminous turbulent flames. The soot depth, $\delta_S$, was measured very simply by inserting arrays of 5 mm diameter glass rods into the flame perpendicular to the wall surface and rapidly withdrawing them after a two second exposure. Megaridis and Dobbins [4] showed that the amount of soot deposited is proportional to the local soot volume fraction in the gas phase. Soot is deposited by action of thermophoresis. The rate of soot deposition: is driven by the temperature difference between the flame and glass rod, is proportional to the soot volume fraction and is independent of the soot particle size. The glass rods heat up only 20 K during the two second measurement time. Two arrays, each containing five rods, were inserted sequentially for each measurement at heights of 365, 527, 771, 1022 and 1317 mm. See

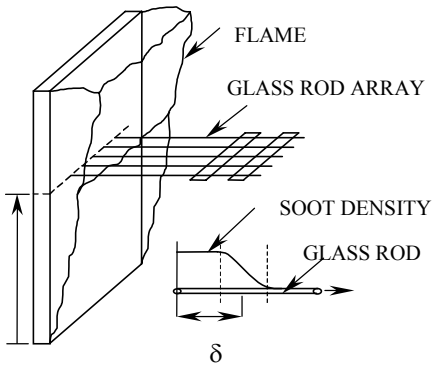


**Figure 2. Sketch and detail of soot depth measurements**

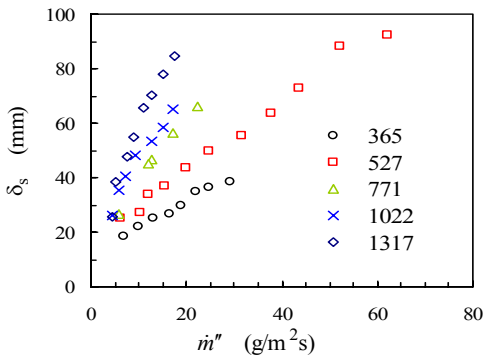


**Figure 3. Measured soot depth, $\delta_s$, vs. fuel mass transfer, $\dot{m}''$, at several heights, z**

Fig. 2. The lowest height of 365 mm insures readings well within the turbulent region. The rods are laterally spaced 41 mm apart and the array was centered on the midpoint of the 380 mm wide burner surface.

The uniformity of the thickness of the soot deposition was judged visually by holding the rod in front of a light source. As shown in Fig. 2, the soot deposition was uniform to the left of the first dotted line and then decreased gradually to zero over a distance about equal to the uniform deposition distance on the left. The soot depth, $\delta_S$, is defined as the distance where the soot deposit is visually judged to have decreased to 50 % of the maximum (e.g. uniform) deposit on that rod. The two-second exposure was chosen on the following basis. A shorter exposure of one second results in intermittent deposition making it difficult to judge any distance. Conversely, longer exposures of four to six

seconds give a uniform heavy deposition that is biased to extra large values of $\delta_S$. The average value of $\delta_S$ is insensitive to exposure times that are near two seconds. Each indicated data point was the average of the 10 readings (2 arrays of 5 rods each). Typically, the standard deviation of the ten individual soot lengths was 10 % of their averaged value so that the estimate of the averages has a 3.4 % standard deviation.

Figure 3 shows the variation of soot depth, $\delta_S$, with mass transfer rate, $\dot{m}''$, at various heights. The data of Fig. 3 apply only to luminous turbulent flames. The luminosity comes from the soot in the flames. For mass transfer rates less than 4 g/m2s the flames became non-luminous and blue[3]. At these very low mass transfer rates the thickness of the blue flames as well as the total heat transfer become independent of height. The data and correlations presented in this paper are for mass transfer rates greater than 4 g/m$^2$ and do not apply to the blue flame regime.

Figure 4 shows the correlation of normalized soot depth, $\delta_S / z$, by the fuel to air mass ratio, $\Psi$, of the luminous turbulent flames. The fuel to air mass ratio, $\Psi$, is proportional to the total fuel supplied up to a given height divided by the accumulated entrainment of air up to the same height. As shown later in Fig. 10, the maximum mean upward velocity is insensitive to the fuel mass transfer and correlates according to $u_{\max} = 0.95\sqrt{2gz}$. According to Taylor's entrainment concept [5], the local air entrainment, $\dot{m}''_{air}$, into the flames is proportional to this upward velocity, $\dot{m}''_{air} \propto \rho_A \sqrt{2gz}$, where $\rho_A$ is the density of ambient air. [Strictly speaking, the entrainment is slightly dependent on the boundary layer width, which in turn depends on $\Psi$.] The integral of the entrainment into the flame boundary layer up to height $z$ is proportional to $\rho_A \, z\sqrt{2gz}$. This is to be compared to the stoichiometric air requirement equal to the sum of all the fuel supplied up to height z multiplied by the stoichiometric oxidant to fuel mass ratio, $s$. So that the relative richness is proportional to

$$\Psi = \frac{s\int_0^z \dot{m}'' dz}{\rho_A \, z\sqrt{2gz}} \tag{1}$$

The correlation gives the empirical formula (solid line) for the flame thickness,

$$\frac{\delta_S}{z} = 0.32\left(\Psi - \Psi_0\right)^{1/2} \quad with \quad \Psi_0 = 0.006 \tag{2}$$

This formula says that the soot depth disappears as $\Psi \to \Psi_0$ for all heights, $z$, in the pyrolysis zone. Indeed, the flames turn blue near this limit. The above formula applies to the turbulent region. Theoretical arguments say that the flame thickness, $\delta_S$, increases with the ¼ power of $z$ in the laminar zone near the leading edge [6]. One can thus extend the soot depth formula to the laminar region by

$$\frac{\delta_S}{z} = \left[1 + \left(\frac{z_t}{z}\right)^9\right]^{1/12} \left[0.32\left(\Psi - \Psi_0\right)^{1/2}\right] \tag{3}$$

where $z_t = 110$ mm is a nominal laminar to turbulent transition height. This correction has negligible effect on $\delta_S$ for $z \geq z_t$ in the turbulent zone.

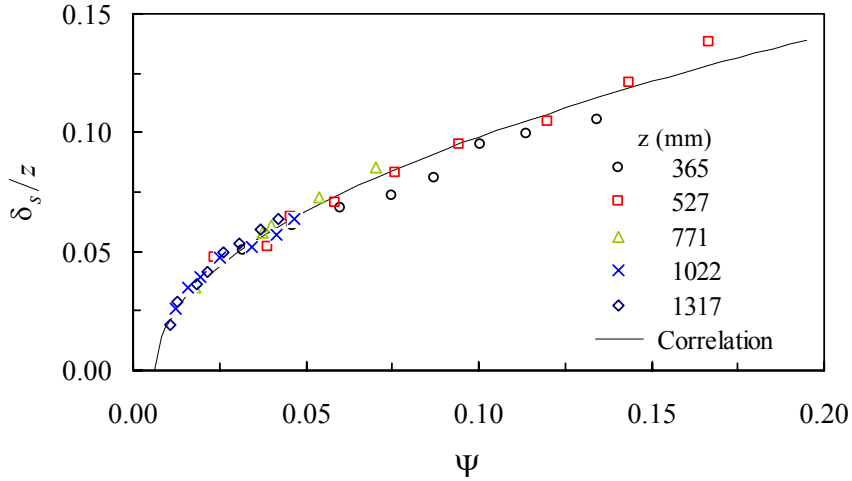


**Figure 4 Correlation (solid line) of measured (symbols) normalized soot depth, $\delta_s/z$, vs. relative fuel richness, $\Psi$, at different heights, z.**

The correlation, Eq. 3, is based entirely on data from the pyrolysis zone. Never the less, it is curious to note that setting $\Psi = \Psi_0$ in Eq. (1) also gives the overall turbulent flame height, $z_f$, in meters, for a line fire against a wall

$$z_f = \left[\frac{s\dot{M}'_f}{\Psi_0\,\rho_A\sqrt{2g}}\right]^{2/3} = \left[\frac{s\dot{Q}'}{\Psi_0\,\Delta H_c\,\rho_A\sqrt{2g}}\right]^{2/3} = 0.047\left[\dot{Q}'\right]^{2/3} \quad (4)$$

for typical fuels releasing $\Delta H_c / sY_{O\infty} = 13.2$ *kJ/g* of O2 consumed with theoretical heat release rates per unit width, $\dot{Q}'$, in kW/m, and the constant 0.047 in units of $m(kW/m)^{2/3}$. This expression compares favorably with Ahmed's empirical correlation [7], $z_f = 0.052\left[\dot{Q}'\right]^{2/3}$, of visible flame heights against a wall. Thus in both cases when $\Psi = \Psi_0$, the abundance of air is sufficient to cause the disappearance of luminous flames

**TEMPERATURE**

A thermocouple rake measured the temperature profile across the flame boundary layer. The rake consisted of 15 ungrounded Chromel-Alumel thermocouples inside 1.6-mm Inconel sheaths protruding 1.5 cm downward into the rising flow. The rake was oriented in a horizontal plane such that the thermocouple spacing was 7.1 mm normal to the wall. After an initial transient, the mean temperature showed no sign of drift, suggesting that soot deposits did not influence them over the measurement period. The temperatures were time-averaged over 95 seconds.

Thermocouples are often used to measure local gas temperatures both inside and near a flame. However, radiation heat loss from thermocouples significantly depresses measured temperatures inside the flame, while radiation from the flame significantly increases the measured temperatures outside the flame. Correction of these effects was performed from our detailed knowledge of the radiation field together with a simple heat transfer model, summarized below.

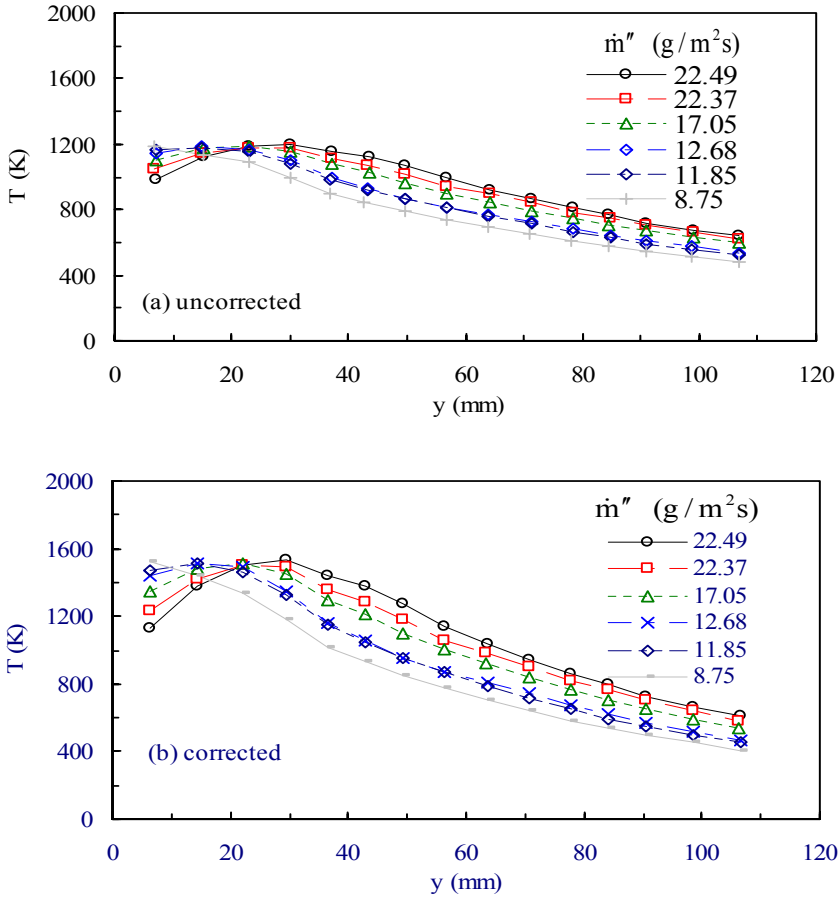


**Figure 5. Temperature, *T*, vs. standoff, *y*, for various propylene mass transfer rates, $\dot{m}''$, at z = 771 mm from the leading edge: (a) uncorrected, and (b) corrected.**

Figure 5(a) shows the uncorrected measured temperature at a height $z = 771\,mm$ for various mass transfer rates, while Figure 5(b) shows the corresponding corrected temperature profiles.

In steady state, the convective heat transfer to the thermocouple from the gas flowing over the thermocouple must equal the radiative heat loss from its surface minus the rate of heat gain by radiation from nearby flames, or

$$h\left(T_g - T\right) = \sigma\left(T^4 - T_\infty^4\right) - \varepsilon_t \varepsilon_f \sigma\left(T_f^4 - T_\infty^4\right) \tag{5}$$

per unit thermocouple surface area. Here $T, T_g, T_\infty$ and $T_f$, respectively, are the thermocouple, gas, ambient and effective flame radiation temperatures, $h$ is the convective heat transfer coefficient, $\sigma$ is the Stefan-Boltzmann constant and $\varepsilon_f(y)$ is the average flame emissivity as viewed by the thermocouple at location $y$. It was implicitly assumed that the thermocouple was coated with a thin layer of black soot causing it to have unit surface absorptivity and emissivity, $\varepsilon_t = 1$. Solving for $T_g$, one has

$$T_g = T + \frac{\sigma}{h}\left(T^4 - T_\infty^4\right) - \frac{\varepsilon_f(y)}{h}\sigma\left(T^4 - T_\infty^4\right) \tag{6}$$

The convective heat transfer coefficient is obtained from the Nusselt number [8]

$$h = \frac{N_u \kappa}{d} \cong \frac{4\kappa_\infty}{d}\left(\frac{T}{T_\infty}\right)^{4/5} = 100\left(\frac{T}{T_\infty}\right)^{4/5} \quad W/m^2K \tag{7}$$

that takes into account the temperature dependence of the gas thermal conductivity, $\kappa_\infty$.

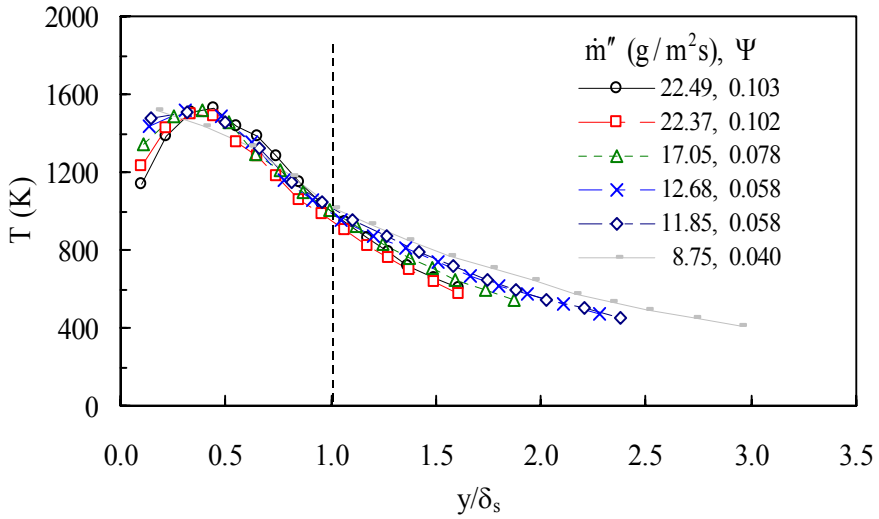


Figure 6 Corrected temperature, T, vs. normalized distance, $y/\delta_S$, for various propylene mass transfer rates, $\dot{m}''$, *at* $z = 771\,mm$ from the leading edge.

The flame emissivity $\varepsilon_f(y)$ was calculated from the sum of the inward and outward directed radiant fluxes coming from a uniform slab of flame having measured: effective flame temperature, $T_f = 1375\,K$, thickness, $\delta_S$, and optical thickness of the various propylene flames [1]. The detailed knowledge of the radiation field produced by these propylene flames makes it possible to accurately calculate these radiation corrections.

Figure 6, above, shows the corrected temperatures plotted instead against $y/\delta_S$. The

temperatures are well correlated inside the flame envelope. That is, the temperature profile inside the flame is largely independent of the fuel to air ratio, $\Psi$. In particular, the temperature at the flame boundary $y = \delta_S$ remains around 1000 K for all values of relative richness, $\Psi$. The similarity correlation is excellent within $0.25 \le y/\delta_S \le 1.5$, but not as good outside these limits. For leaner flames, i.e. flames having lower values of $\Psi$, the temperatures are slightly higher at larger values of $y/\delta_S$ but lower for smaller values of $y/\delta_S$. The similarity applies to the buoyant turbulent combustion controlling the basic combustion process, in the neighborhood of $y \approx \delta_S \propto z(\Psi - \Psi_0)^{1/2}$. Away from the central zone, near the wall the laminar sub-layer tends to be independent of height, whereas far from the wall the turbulent flow scales more nearly according $y \propto z$. As shown later, this same lack of perfect similarity occurs for the velocity profiles.

**RADIANCE**

Measurements [1,3] of the local outward radiance also support the similarity concept. Here the outward radiance is defined as the radiant flux per unit solid angle in the outward normal direction. Scanning radiometer measurements were averaged at the mid-height of each 132-mm high burner segment. Figure 7 shows the outward radiance from the flames vs. mass transfer at four different heights. Radiation comes only from the flames (i.e. the water-cooled sintered-metal burner emits negligible radiation.)

In the case of propylene radiation comes almost entirely from soot. More specifically, the radiance depends on the effective flame radiation temperature, $T_f$, the soot depth, $\delta_S$ and the absorption coefficient. The effective flame radiation temperature was measured by comparing the radiant emission from the flames to the absorption of externally imposed radiation. The comparisons were made for radiation at the same wavelength. Measurements at both 0.9 and 1.0 $\mu m$ wavelengths yielded the same effective flame radiation temperature, $T_f = 1375\ K$ [1]. In addition to being independent of wavelength, $\lambda$, the effective temperature of these propylene flames was independent height, $z$ and mass transfer rate, $\dot{m}''$. This invariance is, indeed, welcome. It simplifies the interpretation of data and development of models. Making the usual assumption that the soot absorption coefficient $\alpha_\lambda = kf_v/\lambda$, varies inversely with wavelength, $\lambda$, it is shown [9] that the radiance, $N_r$, from a homogeneous cloud of soot having volume fraction, $f_v$, and depth, $\delta_S$, is given by

$$N_r(T_f, f_v, \delta_S) = \frac{\sigma T_f^4}{\pi}\left[1 - \frac{15}{\pi^4}\psi^{(3)}\left(1 + \frac{kf_v\delta_S T_f}{C_2}\right)\right] \qquad (8)$$

where $\sigma$ is the Stefan-Boltzmann constant, $C_2$ is Plank's second constant, $k = 8.6$, is the soot extinction constant [10] and $\psi^{(3)}(1+x)$ is the Pentagamma function [9]. The expression, $\frac{15}{\pi^4}\psi^{(3)}(1+x)$, can be conveniently approximated [11] by $\exp(-3.6x)$, to yield

$$N_r\left(T_f, f_v, \delta_S\right) = \frac{\sigma T_f^4}{\pi}\left[1 - \exp\left(-\frac{3.6 k f_v \delta_S T_f}{C_2}\right)\right]. \qquad (9)$$

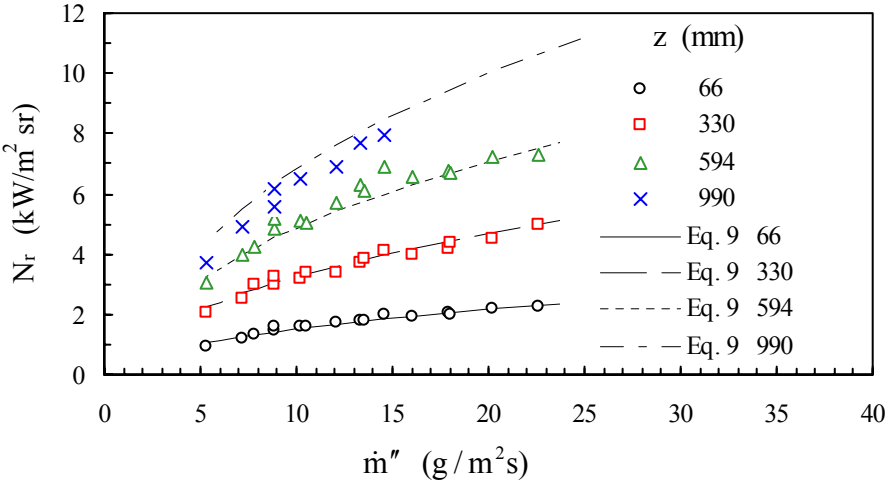


Figure 7. Measured and modeled flame radiance, $N_r$, vs. mass transfer, $\dot{m}''$, at four heights, z, for propylene.

Finally, upon rearranging Eq. (9), $\frac{3.6 k f_v \delta_S T_f}{z C_2} = -\frac{1}{z}\ln\left(1 - \frac{\pi N_r}{\sigma T_f^4}\right)$ and substituting for $\delta_S$ from Eq. (3), one has

$$Y \equiv -\ln\left(1 - \frac{\pi N_r}{\sigma T_f^4}\right) \Bigg/ z\left[1 + \left(\frac{z_t}{z}\right)^9\right]^{1/12} = \frac{3.6 k f_v \left[0.32\left(\Psi - \Psi_0\right)^{1/2}\right] T_f}{C_2} \equiv Y_1 \qquad (10)$$

The radiance measurements are plotted against $\Psi$ in Fig. 8 using the formula for Y together with an effective flame temperature $T_f = 1375\,K$ and laminar to turbulent transition height, $z_t = 0.11 m$. The correction for the laminar flame at the leading edge $\left[1 + \left(\frac{z_t}{z}\right)^9\right]^{1/12}$ becomes important only at the lowest height of 66 *mm* height. As expected the radiance increases approximately with the ¼ power of height, *z*, from the leading edge. The "model" curve in Fig. 8 is obtained from Eq. (10) using $k f_v = 6.9 \times 10^{-6}$ for the present propylene flames [1]. The correlation and model fit are excellent yielding further substantiation for the proposed similarity. The outward radiance also correlates simiarly for methane, ethane and ethylene flames [13].

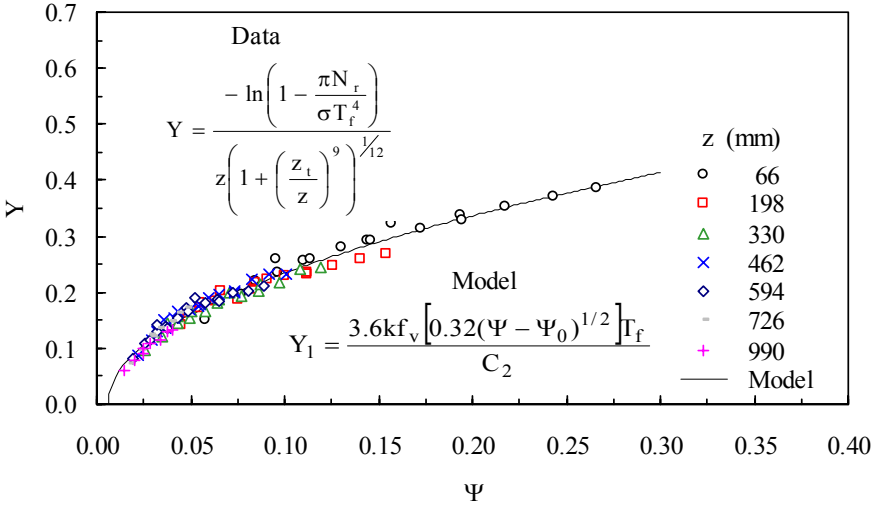


Figure 8. Correlation of measured radiance data, Y, vs. fuel to air ratio, Ψ, for propylene flames at various heights, z, and mass transfer rates. Solid line is Eq. (10).

VELOCITY

Most, Sztal and Delichatsios [12] measured the velocity and temperature profiles of vertical turbulent ethane wall fires. The measurements were performed at FM Global

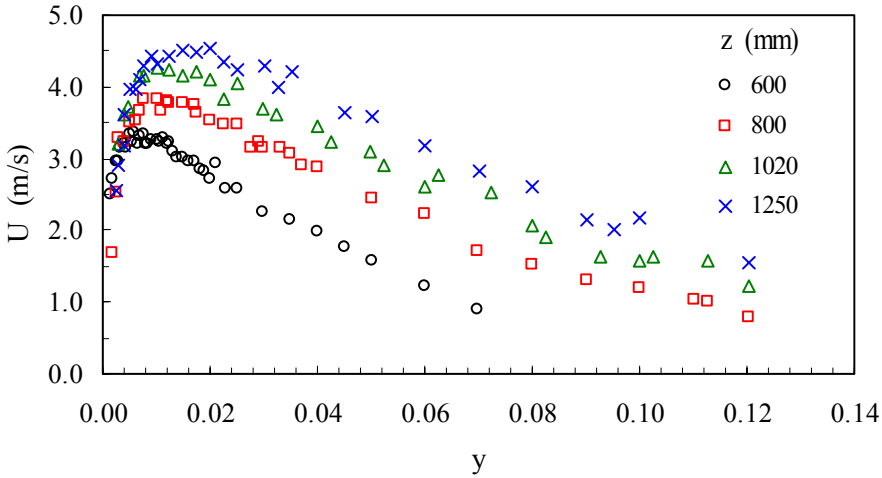


Figure 9. LDV measurements of vertical velocity, U, vs. normal distance, y, for different heights, z, from the leading edge at a mass transfer rate, $\dot{m}'' = 5.4\ g/m^2 s$.

during the summer of 1982. The measurements were not correlated at the time. The

temperature measurements are very similar to those of Fig. 5(b). Now, with the present approach, both the velocity and temperature profiles can be successfully correlated. The temperature correlation is equally as good as shown in Fig. 6. Figure 9 shows the measured upward LDV velocities, U vs. distance, y, at different heights, z, for ethane flames supplied by a mass transfer rate $\dot{m}'' = 5.4\, g/m^2 s$. Figure 10 shows the same data correlated as $U/(2gz)^{1/2}$ *vs.* $y/\delta_S$. The good correlation of both temperature and velocity lends support to the similarity hypothesis of this paper. Careful examination of the temperature and velocity correlations shows the curves for $y/\delta_S > 2.0$ decreasing slightly with increasing relative fuel richness, $\Psi$. Similarly, there is a consistent lack of similarity among the curves for $y/\delta_S < 0.25$. The similarity identified here applies to the main combustion process.

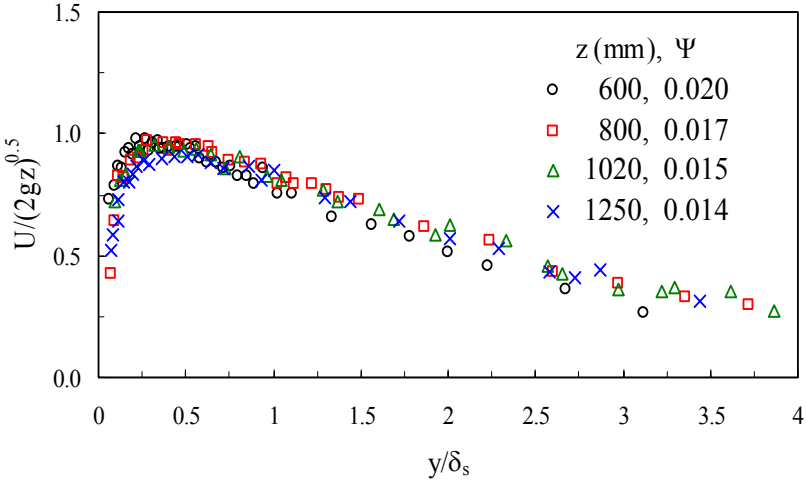


**Figure 10. Correlated velocity, $U/(2gz)^{0.5}$ vs. normalized distance, $y/\delta_s$, for different heights, z, at mass transfer rate, $\dot{m}''$ = 5.4 g/m$^2$s**

## CONCLUSIONS

The relative fuel to air mass ratio, $\Psi$, successfully correlates the: flame thickness, outward directed radiance, and both temperature and velocity profiles across the turbulent boundary layer adjacent to the pyrolysis zone of wall fires. These similarity relationships should simplify the development of both CFD and analytic models of upward burning wall fires.

[1] de Ris, J. L., Markstein, G. H., Orloff, L. and Beaulieu, P. A., Flame Heat Transfer Part I: Pyrolysis Zone, Factory Mutual Research Tech. Report J. I. 0D0J9.MT, September 1999.

[2] Markstein, G. H. and de Ris, J., "Wall Fire Radiant Emission - Part 1: Slot Burner Flames Comparison with Jet Flames," Proc. Combust. Inst. 23, 1685-1692, (1990).

[3] Markstein, G. H. and de Ris, J., "Wall-Fire Radiant Emission – Part 2: Radiation and Heat Transfer from Porous-Metal Wall Burner Flames," *Proc. Combust. Inst. 24*, 1747-52, (1992).

[4] Megaridis, C. M. and Dobbins, R. A., "Soot Aerosol Dynamics in a Laminar Ethylene Diffusion Flame *Proc. Combust. Inst. 22*, 353-62, (1989).

[5] Morton, B. R., Taylor, G. I. and Turner, J. S., "Turbulent Gravitational Convection from Maintained and Instantaneous Sources," *Proc. Roy. Soc.* **A 234,** 1 (1956).

[6] Kim, J. S., de Ris, J. L. and Kroesser, F. Wm., "Laminar Free-Convective Burning of Fuel Surfaces," *Proc. Combust. Inst. 13*, 949-961, (1971).

[7] Ahmed, T., "Investigation of the Combustion Region of Fire-Induced Plumes Along Upright Surfaces," Ph.D. Thesis, Pennsylvania State University, (1978).

[8] Eckert, E. R. G. and Drake, R. M., *Analysis of Heat and Mass Transfer,* McGraw-Hill, 1986

[9] Siegel, R. and Howell, J. R., *Thermal Radiation Heat Transfer, 3rd Ed.,* Hemisphere Publishing Co. (1992).

[10] Choi, M. Y., Mulholland, G. W., Hamins, A. and Kashiwagi, T., "Comparisons of the Soot Volume Fraction Using Gravimetric and Light Extinction Techniques*," Combustion and Flame*, **102,** 161-169 (1995).

[11] Yuen, W. W. and Tien, C. L., "A Simple Calculation Scheme for the Luminous Flame Emissivity," *Proc. Combust. Inst. 16*,. 1481-1487, 1977.

[12] Most, J. M., Sztal, B. and Delichatsios, M. A., "Turbulent Wall Fires – LVD and Temperature Measurements and Implications," Presented at the Second International Symposium on Applications of Laser Anemometry to Fluid Mechanics, Lisbon, Portugal, July 2-4, 1984, (Also Factory Mutual Report Number, RC84-PT-11.)